Received: 13 July 2020 | Revised: 22 June 2021 | Accepted: 9 July 2021

DOI: 10.1002/bit.27900

ARTICLE

BIOTECHNOLOGY AND BIOENGINEERING WILEY

Full-length G glycoprotein directly extracted from rabies virus with detergent and then stabilized by amphipols in liquid and freeze-dried forms

Didier Clénet[1] | Léna Clavier[1] | Benoît Strobbe[1] | Christel Le Bon[2] | Manuela Zoonens[2] | Aure Saulnier[1,3]

[1]Bioprocess R&D Department, Sanofi Pasteur, Marcy l'Etoile, France

[2]Laboratoire de Biologie Physico-Chimique des Protéines Membranaires, CNRS, Institut de Biologie Physico-Chimique, Université de Paris, Paris, France

[3]Department of Analytical Sciences, Sanofi Pasteur, Marcy l'Etoile, France

Correspondence
Didier Clénet, Bioprocess R&D Department, Sanofi Pasteur, 69280 Marcy l'Etoile, France.
Email: didier.clenet@sanofi.com

Abstract

Pathogen surface antigens are at the forefront of the viral strategy when invading host organisms. These antigens, including membrane proteins (MPs), are broadly targeted by the host immune response. Obtaining these MPs in a soluble and stable form constitutes a real challenge, regardless of the application purposes (e.g. quantification/characterization assays, diagnosis, and preventive and curative strategies). A rapid process to obtain a native-like antigen by solubilization of a full-length MP directly from a pathogen is reported herein. Rabies virus (RABV) was used as a model for this demonstration and its full-length G glycoprotein (RABV-G) was stabilized with amphipathic polymers, named amphipols (APols). The stability of RABV-G trapped in APol A8-35 (RABV-G/A8-35) was evaluated under different stress conditions (temperature, agitation, and light exposure). RABV-G/A8-35 in liquid form exhibited higher unfolding temperature (+6°C) than in detergent and was demonstrated to be antigenically stable over 1 month at 5°C and 25°C. Kinetic modeling of antigenicity data predicted antigenic stability of RABV-G/A8-35 in a solution of up to 1 year at 5°C. The RABV-G/A8-35 complex formulated in an optimized buffer composition and subsequently freeze-dried displayed long-term stability for 2-years at 5, 25, and 37°C. This study reports for the first time that a natural full-length MP extracted from a virus, complexed to APols and subsequently freeze-dried, displayed long-term antigenic stability, without requiring storage under refrigerated conditions.

KEYWORDS

A8-35 formulation study, amphipol-stabilized integral membrane protein, G glycoprotein from rabies virus, stable freeze-dried A8-35 formulation

Abbreviations: 95% PI, prediction intervals at 95%; A8-35, poly(sodium acrylate)-based amphipol comprising 35% of free carboxylate, 25% of octyl chains, and 40% of isopropyl groups; APols, amphipols; CD, circular dichroism; CHAPS, 3-((3-cholamidopropyl) dimethylammonio)-1-propanesulfonate; CYMAL-6, cyclohexyl-hexyl-β-D-maltosid; DDM, dodecylmaltoside; DF, diafiltration; DoE, design of experiments; DSC, differential scanning calorimetry; ELISA, enzyme-linked immunosorbent assay; HEPES, (4-(2-hydroxyethyl)piperazine-1-ethanesulfonic acid, *N*-(2-hydroxyethyl)piperazine-*N*′-(2-ethanesulfonic acid); ICH, international conference harmonization; mAb, monoclonal antibody; MPs, membrane proteins; nDSF, nano differential scanning fluorimetry; nMOMP, native major outer membrane protein; RABV, rabies virus; RABV-G, rabies virus glycoprotein G; SD, standard deviation; SMA, styrene and maleic acid; Tg, glass transition temperature of the freeze-dried product; TGA, thermogravimetric analysis; Tg′, glass transition temperature of the maximally freeze-concentrated bulk solution surrounding the ice crystals; Tris, Tris(hydroxymethyl)aminomethane); $T_{unf\ II}$, temperature-induced unfolding of secondary structure of RABV-G; $T_{unf\ III}$, temperature-induced unfolding of tertiary structure of RABV-G; UF, ultrafiltration; UVA, ultraviolet radiation with wavelengths between 320 and 400 nm; VIS, visible light, i.e., wavelengths between 400 and 800 nm.

1 | INTRODUCTION

Host antiviral protective immunity is mainly elicited against surface antigens, generally, glycoproteins embedded in the lipid membrane. Even though membrane proteins (MPs) are key antigenic targets, only a few MP-based subunit vaccines have been developed, for example, against hepatitis B (Ionescu-Matiu et al., 1983) or papillomavirus (Suzich et al., 1995). MPs are expressed naturally at low levels in vivo, requiring the use of different production strategies such as recombinant or cell-free systems (Blesneac et al., 2012; Dilworth et al., 2018; Wuu & Swartz, 2008; Zoonens & Miroux, 2010). Moreover, due to their hydrophobic transmembrane region, MPs are not soluble in aqueous media, leading to spontaneous aggregation and loss of activity unless surfactants are used. Removal of the transmembrane region is a strategy commonly used to facilitate the production of soluble ectodomains as recombinant proteins. However, the risks of protein misfolding and loss of antigenicity of truncated-MP versions are high. As it has been already observed for various viral proteins (ebola, rabies, SARS-CoV, influenza, and paramyxoviruses), the transmembrane domain has an impact on protein folding and stability (Ci et al., 2018; Smith et al., 2012, 2013; Webb et al., 2018). In the case of the rabies virus (RABV), the soluble ectodomain of the glycoprotein expressed in eukaryotic cells folds in a monomeric conformation, which is antigenically distinct from the complete native membrane-anchored glycoprotein (Maillard & Gaudin, 2002). These observations suggest that producing full-length MPs is preferable to trigger an antigenic response comparable to that provided by lived pathogens. Mild extraction of full-length MPs directly from viral particles can provide simple access to antigens which comprise all protein domains (the ecto-, transmembrane-, and endodomains) and thus would retain their original antigenic conformation, even if three-dimensional conformations of these MPs exist in a fragile equilibrium of few preferential conformations with close free activation energies (Qoronfleh et al., 2007). In the aim to preserve the native conformation of the target MP, mild surfactants can be used as substitutes for the lipid environment surrounding the transmembrane domain of MPs.

Detergents constitute a large class of surfactants traditionally used to solubilize membranes and to maintain MPs in water-soluble forms (Alberts & Lewis, 2002; Duquesne & Sturgis, 2010; Orwick-Rydmark et al., 2016). The presence of detergents can, however, lead to MP instability, likely due to the detergent binding to and dispersing hydrophobic moieties (e.g., lipids or cofactors), resulting in "poisoning" hydrophobic pockets in MPs, or partial unfolding of native conformers (Otzen, 2015; Zoonens et al., 2013). Alternatives to conventional detergents have emerged. On the one hand, detergent molecules with original chemical structures have been synthesized like, for instance, maltoside derivatives (Sadaf et al., 2015) or calixarenes (Hardy et al., 2016, 2019; Matar-Merheb et al., 2011). These latter have recently been tested in vaccine application against influenza (Mandon et al., 2020). On the other hand, original amphipathic systems have been developed including fluorinated surfactants, nanodiscs, or amphipathic polymers (Popot, 2010). Among the latter, styrene maleic acid (SMA) co-polymers (Dorr et al., 2016; Knowles et al., 2009; Simon et al., 2018; Stroud et al., 2018) and polyacrylic-based amphipols (APols) (Marconnet et al., 2020; Popot et al., 2011, 2018; Tribet et al., 1996) are the most studied and characterized polymers. Presently, APol A8-35 is a useful surfactant substitute to stabilize and preserve the native-like conformation of antigens for their use as controls in characterization assays (Feinstein et al., 2014). APol A8-35 has been functionalized and constitutes a useful tool for detection support (Charvolin et al., 2009; Della Pia, Holm, et al., 2014; Giusti et al., 2015; Le Bon et al., 2014). Furthermore, protection against *Chlamydia muridarum* in a murine model using A8-35 as a delivery vehicle of antigens has been reported (Della Pia, Hansen, et al., 2014; Tifrea et al., 2011, 2018, 2020).

The RABV transmembrane glycoprotein G (RABV-G) was chosen as a model of viral MPs. RABV-G is a 505-amino acid long MP (UniProtKB - P15199) that crosses the viral lipid membrane with a single transmembrane α-helix of 21 amino acids (460–480). RABV-G is involved in the initial steps of virus binding to cell receptors and thereafter triggers uncoating and genome delivery due to low pH-induced membrane fusion within the endocytic pathway (Belot et al., 2019). Sequence alignment with G of vesicular stomatitis virus showed that RABV-G likely adopts the typical fold of Class III fusion glycoproteins. The glycosylation sites are located in the ectodomain exposed at the surface of the virus and one lipidation site is located close to the transmembrane domain. At the surface of the virion, a pH-dependent equilibrium has been described between the pre- and postfusion conformations of G protein and monomeric intermediates during the structural transition (Albertini et al., 2012).

The aim of the present study was to develop a simple and straightforward method to isolate and stabilize a full-length MP from a pathogen that would be antigenically similar to the MP located at the surface of the pathogen. RABV-G was used as a model for this demonstration. The protein was first solubilized in detergent and subsequently complexed to APol A8-35. The stability of the soluble RABV-G was physically and biochemically evaluated (e.g., antigen structure and aggregation state) under various stress conditions such as high temperature (up to 37°C), agitation, and light exposure. Finally, a formulation development study was conducted to identify the best buffer composition for a freeze-drying process of the RABV-G antigen to propose a format that permits long-term storage.

2 | MATERIALS AND METHODS

2.1 | Rabies virus

Bulk RABV, from the original Wistar Rabies Pitman Moore/WI 38 1503-3M strain, was produced in Vero cells, inactivated with β-propiolactone and purified. RABV was stored frozen below −70°C and thawed overnight under refrigerated conditions before use. RABV was chosen as a model in this study.

2.2 | Extraction, purification, and formation of G protein/A8-35 complex

About 500 ml of a RABV bulk were 10-fold concentrated by ultrafiltration (UF) with a Labscale TFF System (Millipore), using a UF 100 kDa Pellicon XL Biomax type C PES cassette (Millipore). The concentration of total proteins was estimated at 3.4 mg/ml using the Bradford assay. The retentate was diafiltrated (DF) with 20 mM Tris and 150 mM sodium chloride at pH 7.5. Following the addition of 0.6% w/v CHAPS (3-[(3-cholamidopropyl)dimethylammonio]−1-propanesulfonate, Sigma-Aldrich), the solution was incubated overnight (~16 h) at +5°C under slight agitation. The sample was then centrifuged for 20 min. at 12,000 *g*. The supernatant was recovered and poured onto a 5%–20% w/w sucrose gradient. After centrifugation (16 h at 164,100 *g*), the gradient was fractionated (16–17 fractions), and the fraction content was analyzed by sodium dodecyl sulfate-polyacrylamide gel electrophoresis (SDS-PAGE). Fractions containing RABV-G were pooled, submitted to a UF/DF step in 20 mM Tris and 150 mM sodium chloride at pH of 7.5 and adjusted to a final concentration of proteins of 0.3 mg/ml. Then, a concentrated stock solution of A8-35 (Anatrace) was added under gentle agitation to the RABV-G/CHAPS solution at 2:1 w/w amphipol:protein ratio and incubated at +5°C for 20 min. Approximately 2 g of polystyrene Bio-beads™ SM-2 (Biorad) were added to 20 ml protein solution and the samples were incubated for 2.5 h at +5°C, under gentle agitation to remove the detergent. The polystyrene beads settled out and the supernatant containing RABV-G/A8-35 was collected and stored at +5°C.

2.3 | Formulation

Di-hydrate trehalose at 100 g/L (292 mM), a lyoprotectant, was integrated into the RABV-G/A8-35 formulation aiming to evaluate buffer, pH, and ionic strength on antigen stability. Tris (2-amino-2-(hydroxymethyl)−1,3-propanediol, THAM, Tris base, Tris(hydroxymethyl)aminomethane, Sigma-Aldrich) and HEPES (4-(2-hydroxyethyl)piperazine-1-ethanesulfonic acid, *N*-(2-hydroxyethyl) piperazine-*N*′-(2-ethanesulfonic acid, Sigma-Aldrich) buffers (20 mM) were chosen to respect the basic pH compatibility of A8-35 and to ensure buffering effect within the pH ranges of 7.5–8.5 and 7.0–8.0, respectively. Ionic strength impact was evaluated by adding sodium chloride up to 6 g/L (103 mM). Central composite designs (design of experiment [DoE]) combining two continuous factors, pH and sodium chloride concentrations, and including two central points were built in JMP (V. 11, SAS Institute Inc.) software, for statistical analysis. This DoE comprised of 10 Tris/trehalose-based formulations and 10 HEPES/trehalose-based formulations with sodium chloride ranging from 5 mM to 103 mM to evaluate impact of pH ranging 7.0–8.5 and ionic strength on RABV-G/A8-35 stability (Table S1).

A CM3-Freeslate (Unchained Labs) robot was used to automatically mix 3–10-time concentrated stock solutions in 10 ml neutral glass vials and to prepare the 20 formulations. Target pH of the formulations was adjusted by adding chloride acidic (1 N) in Tris-based formulations and sodium hydroxide (1 N) in HEPES-based formulations, based on volumes determined by using CurTiPot free software (version 4.2.3, Ivano G. R. Gutz ed.). Buffer exchange of RABV-G/A8-35 at 0.3 mg/ml in Tris/NaCl buffer against these 20 formulations was carried out on Amicon® centrifugal filter units (50 kDa cut-off). The 1 ml of RABV-G/A8-35 solutions were 10-time diluted by the formulations in 20 centrifugal filter units, then concentrated (centrifugation at 3000 *g*, 5 min.). Final volumes were adjusted to get 1 ml of RAVB-G/A8-35 at a final protein concentration of 0.3 mg/ml in each of the 20 formulations.

Impact of buffer/pH and ionic strength on RABV-G/A8-35 stability was evaluated at time-zero by determination of the antigen unfolding temperature ($T_{unf.III}$) by nano-differential scanning fluorescence (nDSF) and, after incubation of samples 24 h at 45°C, through turbidity measurements at 320 nm absorbance, and antigenicity by dot blot. In addition, the critical glass transition temperature of the maximally freeze-concentrated bulk solution surrounding the ice crystals (Tg′) was also determined for each formulation. Statistical analysis of data was performed using JMP software. Differences were determined to be significant when the probability of chance explaining the results was reduced to less than 5% ($p < 0.05$). The results of the formulation study were used to derive an optimal formulation for the freeze-drying process.

2.4 | Buffer exchange and freeze-drying processes

Diafiltration of 50 ml RABV-G/A8-35 at 0.3 mg/ml in Tris/NaCl buffer against the selected formulation was carried out using a Labscale diafiltration unit (Millipore) with a Pellicon XL Biomax 50 kDa cassette. The formulated RABV-G/A8-35 samples (0.5 ml) were filled in 3 ml TopLyo (Schott) vials which were half-stoppered and loaded onto the shelf of the Lyovac FCM 10 (GEA) freeze-dryer. From room temperature, samples were initially frozen at −50°C for 1.5 h, followed by an isothermal stage for 1 h. For the primary drying step, the shelf temperature was increased to −30°C over 0.5 h while decreasing the chamber pressure to 0.05 mbar and then maintained at −30°C for 33.3 h during primary drying. The secondary drying step was performed by further increasing the shelf temperature to +33°C over 5 h while maintaining the chamber pressure to 0.05 mbar, followed by 10 h drying at +33°C. At the end of the cycle, the vials were closed under nitrogen at 800 mbar, sealed with aluminum caps and stored at +5°C or incubated at +25°C or +37°C for stress testing. Freeze-dried products were reconstituted with 0.5 ml of sterile water before testing (antigenicity, pH, and turbidity).

2.5 | Thermal stress

Liquid samples were aliquoted in 1.8 ml polypropylene cryotubes (Nunc) and maintained independently for 7, 14, and 29 days at 5°C or 25°C or for 1, 2, or 7 days at 37°C. Freeze-dried samples were

maintained in 3 ml type I glass vials (Schott) for up to 2 years at 5°C, 25°C, or 37°C.

2.6 | Mechanical stress

Liquid samples were added to 3 ml type I glass vials (Schott) and submitted to stirring stress using magnetic bars on a CM3-Freeslate stirring deck (Unchained Labs). Stirring ensuring a turbulent flow at 550 rpm was used to trigger a progressive and continuous protein aggregation. This mechanical stress was carried out for 2 h or 6 h at room temperature.

2.7 | Photostability: Light exposure

RABV-G/A8-35 liquid samples in type I glass vials (Schott) were exposed to UVA (320–400 nm, doses: 200 and 400 Wh/m²) and visible light (VIS, 400–800 nm, doses: 708 and 1674 klux-hour) in a Caron 6540 photoluminescence chamber at 15°C. The experiment total duration was 4 days. Negative control and lower dose samples were protected from light exposure with aluminum foil. After each type of stress, samples were aliquoted, instantly frozen and stored at −70°C until analysis.

2.8 | Total protein quantification and turbidity of RABV-G solution

UV absorbance of the samples (250 µl) was measured with SpectraMax M5 UV-visible spectrophotometer (Molecular Devices®). Independent wavelength measurements were performed at 280, 320, 350, and 975 nm, using the "pathcheck" function to normalize measurements. Concentration of the RABV-G protein was estimated based on a mass extinction coefficient of 1.4562 ml mg^{-1} cm^{-1} at 280 nm (estimated with ExPASy Prot Param software), after correction of light scattering contribution using the samples' absorbance at 350 nm. The presence of insoluble aggregates in formulations of RABV-G was estimated through determination of turbidity by measuring the absorbance at 320 and 350 nm.

2.9 | RABV-G thermal unfolding temperatures

Tertiary structure unfolding temperatures ($T_{unf.III}$) were assessed using intrinsic tryptophan fluorescence of proteins by applying Nano Differential Scanning Fluorimetry, nDSF (Prometheus NT.48 instrument, NanoTemper Technologies GmbH). Duplicate RABV-G samples were analyzed in high sensitivity (HS) capillaries (NanoTemper), after a 1:2 dilution in their respective formulation buffer. During analyses, intrinsic fluorescence emission intensities at the single wavelengths of 330 nm and 350 nm were recorded while samples were heated from 15°C to 95°C at 1°C/min. The ratio of 350/330 nm intensities was recorded as a function of temperature to define when thermal protein unfolding happens: $T_{unf.III}$ was determined as the temperature at the maximum first derivative of this thermal trace. $T_{unf.III}$ was determined at ±1°C, based on experimental reproducibility results.

2.10 | RABV-G secondary structure

The RABV-G samples were dialyzed with a Slide-A-Lyzer™ cassette (Thermo Fisher Scientific) against a 20 mM Tris, 150 mM NaF, pH 7.5 containing 0.6% CHAPS or 0.06% A8-35 solution. Circular Dichroism (CD) analysis was performed with a J-1500 spectropolarimeter (JASCO, Inc.), and the CD spectra were measured between 190 and 250 nm, with a 0.5 nm interval. The percentage of the structural conformations was calculated by using the free software package CDPro. Thermal denaturation of sample was carried out with a ramp of 1°C/min., between 20°C and 96°C. CD spectra were recorded every 2 min. The melting temperature ($T_{unf.II}$) of the RABV-G was determined as the temperature at the maximum first derivative of the change of ellipticity at 222 nm.

2.11 | SDS-PAGE and western blot RABV-G characterization

Sample protein electrophoresis was performed onto tricine-SDS-PAGE 4-15% gel Criterion™ TGX™ (BioRad), in TGS buffer. Approximately 3 µg of total proteins were heated 5 min. at 100°C before loading for analysis. In addition, RABV was also analyzed under reductive conditions in 20 mM DTT in Laemmli Sample Buffer (BioRad), before heating and loading. Precision Protein STD unstained kit (BioRad) was used as a molecular weight marker. Proteins were stained with Bio-safe Coomassie (BioRad) and analyzed through GS-800 imaging densitometer (BioRad) and its dedicated QuantityOne software. Protein purity was calculated using Un-Scan-It (Silk Scientific. Inc.) software. After the protein gel separation, a western blot was performed on the polyvinylidene difluoride membrane; the conformational monoclonal antibody (mAb) D1-25, specific for a conformational epitope of antigenic site III of RABV- G was used to detect the different RABV-G products by using a Li-Cor Odyssey® instrument.

2.12 | RABV-G antigenicity

Anti-G specific ELISA was performed as previously described (Chabaud-Riou et al., 2017), after demonstrating beforehand that APols have no interfering effect on testing.

For dot blot analyses, 50 ng of samples were spotted onto 0.22 µm nitrocellulose membrane (Invitrogen), using Bio-Dot™ apparatus (Bio-Rad). The mAb D1-25, specific for a conformational epitope of antigenic site III of RABV-G was used for primary hybridization of the dot blot membrane and the secondary antimouse

DyLight800 (Rockland Immunochemicals) antibody for detection. Fluorescence intensities at infrared 800 nm were measured with an Odyssey® fluorimeter (Li-Cor Biosciences) using acquisition software Odyssey Infrared Imaging System v.3.0.21.

2.13 | Glass transition temperatures of RABV-G solutions and freeze-dried products

A power compensation calorimeter equipped with an Intracooler II (DSC8500; PerkinElmer) was used to determine critical process temperatures namely the glass transition temperature of the maximally freeze-concentrated bulk solution surrounding the ice crystals (Tg′) and the glass transition temperature (Tg) of amorphous materials (freeze-dried product). The sample (approximatively 10 µl of solution or 2 mg of dried powder) was sealed in an aluminum pan (with hole for powders) and an empty pan was used as reference. Liquid samples were cooled to −60°C to ensure temperature stability and sample equilibration and scanned at 5°C/min. to 25°C. Tg′ determinations were done on the heating scan. Solid samples were heated from 20°C to 150°C. The first scan removed residual water and the second heating scan was performed at 5°C/min. was used to determine Tg of dried powders. Such values were used to estimate the impact of formulation compositions. All glass transition (Tg′ and Tg) values were reported as the midpoint temperature of the heat capacity step associated to the glass transition. The Pyris (PerkinElmer) software was used to control the instrument and to reprocess the thermograms.

2.14 | Residual moisture content of freeze-dried product

A few milligrams of freeze-dried product were insulated from the ambient atmosphere through crimping of a capsule. A hole was made at the top of the capsule using a needle just before placement in the TGA7 thermogravimetric analyzer (PerkinElmer). The sample was subjected to a temperature increase of 5°C/min. between ambient temperature and 250°C. The water content was measured as the loss of mass observed up to about 110°C. The Pyris (PerkinElmer) software was used to extrapolate residual moisture from the thermograms.

2.15 | Advanced kinetics modeling and stability predictions of RABV-G

Taking 1-month stability G-specific ELISA data sets obtained at 5°C (standard storage temperature) and also at 25°C and 37°C (accelerated conditions), the AKTS-Thermokinetics software (version 5.1, Advanced Kinetics and Technology Solutions AG, AKTS) was used to develop and implement RABV-G kinetic models and predict loss of antigenicity of RABV-G as a function of temperature exposure in liquid solutions, under isothermal and nonisothermal conditions, as previously described (Clénet, 2018; Roduit et al., 2014; Roque et al., 2021). The 95% percentile bootstrapped confidence intervals were calculated to define the accuracy of predictions which are graphically included as prediction bands.

3 | RESULTS

3.1 | G protein extraction from rabies virus, purification, and trapping in amphipols

Viral proteins were extracted with CHAPS from RABV whole particles. The G protein was purified on sucrose gradient as previously described (Yves Gaudin et al., 1992). After solubilization, the recovery yield of G protein was approximately 70%. The oligomeric forms of the integral G protein in CHAPS (RABV-G/CHAPS) were separated on a sucrose gradient (data not shown) and identified by SDS-PAGE as previously demonstrated (Yves Gaudin et al., 1992). CHAPS was then subsequently exchanged for APol A8-35 as previously reported (Le Bon et al., 2018; Zoonens et al., 2005). The resulting complexes of G protein trapped in A8-35 (RABV-G/A8-35) were water soluble and approximately 90% pure (Figure S1). RABV-G/CHAPS and RABV-G/A8-35 complexes showed a similar antigenicity consistent with the original RABV (Figure S1).

3.2 | Characterization of integral RABV-G protein in solution

The purified full-length RABV-G protein in either CHAPS or A8-35 was characterized under the same experimental conditions, that is, at a protein concentration of 0.3 mg/ml and in buffer containing 20 mM Tris pH 7.5, 150 mM sodium chloride. The protein in the two different surfactants showed similar antigenicity based on G-specific ELISA (Table 1). Solutions looked limpid by eye (i.e., without turbidity) as confirmed by the low absorbance value at 320–350 nm (data not shown). RABV-G exhibited folded secondary structures in both formulations, with approximately 24% of α-helices, 30% of β-sheets, and 12% of β-turns (Table 1). The thermal stability of RABV-G was assessed with the determination of the unfolding temperature values of secondary ($T_{unf.II}$) and tertiary ($T_{unf.III}$) structures using CD and nDSF, respectively (Table 1). Unfolding temperature values were higher for the RABV-G/A8-35 formulation as compared with the RABV-G/CHAPS formulation, indicating higher thermal stability of the APol-associated G protein.

3.3 | Stability of RABV-G in solution

The thermal stability of RABV-G in solution was assessed with the evolution of the antigenicity response and the turbidity of samples incubated over one month at two temperatures, 25°C and 37°C. The

TABLE 1 RABV-G protein characteristics in solution in the presence of either detergent (CHAPS) or amphipol (A8-35)

	Antigenicity (UI/ml) ±95% CI	Secondary struc. by CD	Unfolding temp.Tunf.II by CD (°C)	Unfolding temp.Tunf.III by nDSF (°C)
RABV-G/CHAPS	835 [735–935]	α-helix 24% β-sheet 31% Turn 12% other 33%	49 ± 1	44 ± 1
RABV-G/A8-35	764 [672–856]	α-helix 23% β-sheet 28% Turn 12% other 37%	67 ± 1	50 ± 1

Note: Physical characteristics of RABV-G protein (secondary structures and unfolding temperatures) were measured at a protein concentration of 0.3 mg/ml and in buffer containing 20 mM Tris pH 7.5, 150 mM sodium chloride.

Abbreviations: CD, circular dichroism; CHAPS, 3-((3-cholamidopropyl) dimethylammonio)-1-propanesulfonate; CI, confidence interval; nDSF, nano differential scanning fluorimetry; RABV-G, rabies virus glycoprotein G.

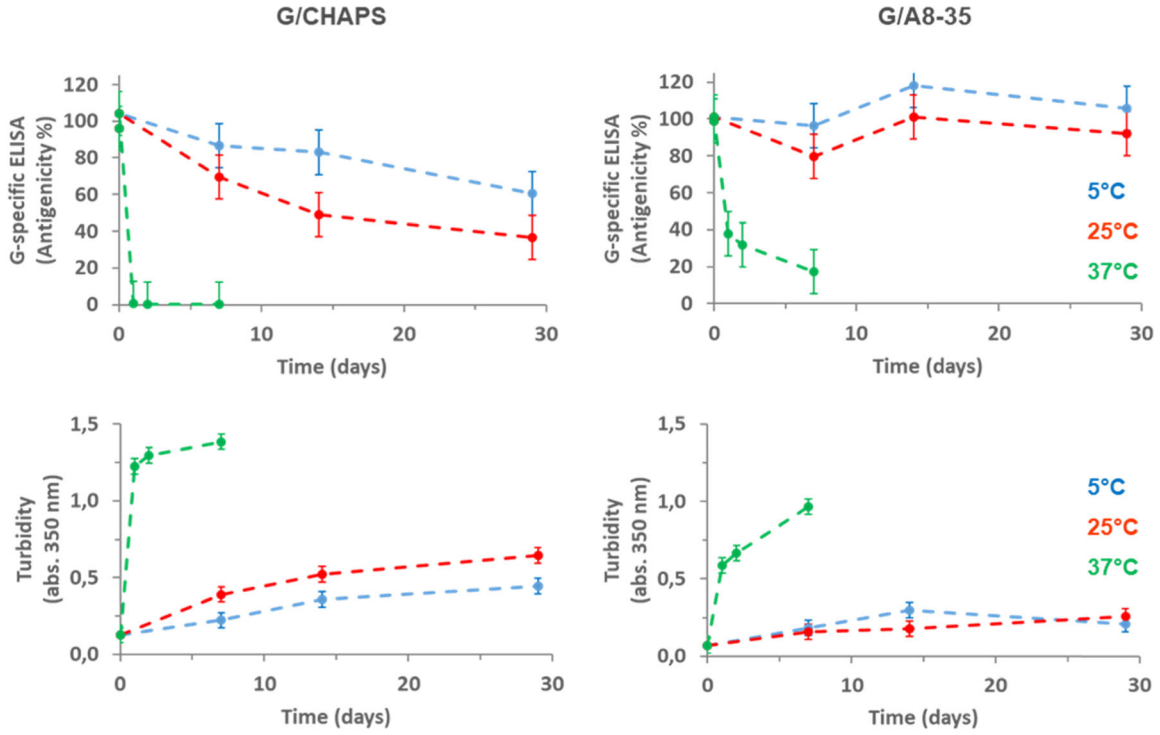

FIGURE 1 Thermal stability of RABV-G/CHAPS (left) and RABV-G/A8-35 (right) formulations: Impact of incubation temperature (5°C in blue, 25°C in red, 37°C in green) on G antigenicity (top) and solution turbidity (bottom). G-specific ELISA timepoints were normalized to initial value (time-zero). Error bars represent 95% CI for ELISA and ±1 ′ for turbidity based on experimental reproducibility results. CHAPS, 3-((3-cholamidopropyl) dimethylammonio)-1-propanesulfonate; CI, confidence interval; ELISA, enzyme-linked immunosorbent assay; RABV-G, rabies virus glycoprotein G; *SD*, standard deviation

data were compared with the samples kept under standard refrigerated storage condition at 5°C (Figure 1).

Irrespective of the incubation temperature, a significant loss of RABV-G antigenicity with a concomitant increase of turbidity was observed for the CHAPS-based formulation. After one month at 5°C and 25°C, approximately 50% of RABV-G/CHAPS antigenicity was lost, whereas the highest incubation temperature (37°C) induced a complete loss of RABV-G/CHAPS antigenicity after 1 day (Figure 1). Conversely, the RABV-G/A8-35 antigenicity was fully preserved over one month at 5°C and 25°C.

Under such storage conditions, increase of turbidity is moderate and is approximately half of that observed in the CHAPS-based formulation (Figure 1). However, significant and rapid loss of RABV-G/A8-35 antigenicity was observed at 37°C with an increase of turbidity, indicating a protein aggregation phenomenon (Figure 1). It is worth noting that the loss of RABV-G specific antigenicity observed at 37°C arose less rapidly in the formulation containing APol than the one with detergent. These data obtained at 5°C, 25°C, and 37°C were used to build a kinetic model enabling to predict the evolution of RABV-G antigenicity at any storage temperature. With this approach, a steady state of the APol-based formulation was predicted over one year at 5°C without significant loss of RABV-G antigenicity, whereas under the same storage conditions, around 70% of RABV-G antigenicity was lost for the formulation containing CHAPS (Figure S2). It should be noted that stability modeling predictions indicated a complete loss of RABV-G antigenicity for both formulations after 1 year when samples are stored at 25°C (Figure S2). It is worth noting that such kinetic models only depict phenomenological models applied for fitting the experimental reaction progress. Nonetheless, it was demonstrated that long-term stability predictions can be done with accuracy since an appropriate kinetic model, that is, describing the degradation progress as a function of time and temperature, was used (Roque et al., 2021), thus reinforcing the best thermal stability predicted for RABV-G formulated with amphipol. Furthermore, simulations from the ELISA kinetic model describing the loss of RABV-G antigenicity upon temperature highlighted an increase of the transition temperature for the APol-based formulation (+5°C) compared to the CHAPS-based formulation, confirming the results observed by nDSF (Figure S3).

The stability of RABV-G/A8-35 in solution was further assessed using either mechanical stress or light exposure. Stirring induced a progressive loss of RABV-G antigenicity as determined by ELISA (~50% of antigenicity was lost after 6 h) with a significant increase of turbidity (Figure 2). Exposures of APol-based formulations to UV-visible wavelengths for several days led to a loss of approximately 50% of RABV-G/A8-35 antigenicity, but without protein aggregation (Figure 2). Note that similar results were obtained for RABV viral particle suspension (data not shown).

Finally, the presence of APol A8-35 improved the thermal stability of RABV-G as compared with the detergent-based formulation, but RABV-G was still sensitive to mechanical or light stress. With the aim of preventing stability issues inherent to MPs in aqueous solutions, a solid form obtained by a freeze-drying process was considered.

3.4 | Ultra-stable amphipol-G protein complexes under freeze-dried form

RABV-G/A8-35 formulation was first optimized through screening of buffer composition (pH and ionic strength). A surface response DoEs (central composite) was built with Tris and HEPES buffers to cover a pH range from 7.0 to 8.5, in the presence of increasing concentrations of sodium chloride (from 5 mM to 103 mM). Trehalose, at a fixed concentration, was systematically added as a common bulking agent to the buffers, yielding 20 different formulations (Table S1). Glass transition temperatures of the maximally freeze-concentrated solutions (Tg′) as well as unfolding temperatures of tertiary structure ($T_{unf.III}$) of RABV-G/A8-35 were determined in each formulation by DSC and nDSF, respectively. Furthermore, after incubation at 45°C for 2 days of the 20 formulations, the turbidity (at 320 nm) and loss of RABV-G/A8-35 antigenicity were monitored.

According to modeling of results in JMP software, appropriate fits were obtained to describe the impact of pH and sodium chloride concentration on Tg′ temperatures (−37°C to −32°C), $T_{unf.III}$ unfolding temperatures (40–55°C), turbidity and antigenicity recovery (Figure S4). In Tris/trehalose-based formulations, increasing pH values significantly enhanced the $T_{unf.III}$ from 37°C to 51°C and antigenicity recovery from 25% to 48%, whereas no significant impact of sodium chloride was observed in the tested concentration range

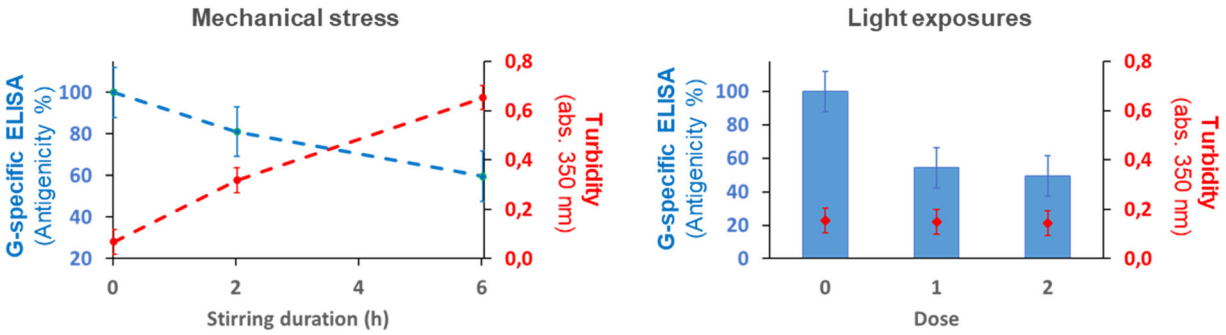

FIGURE 2 Impact of external stresses on RABV-G/A8-35 stability in solution. Mechanical stress (stirring, 550 rpm) and light exposures (dose 0: control, without light exposure; dose 1: UVA 200 Wh/m² + VIS 708 klux·hour for 4 days at 15°C; dose 2: UVA 400 Wh/m² + VIS 1674 klux·hour for 4 days at 15°C) on G antigenicity (blue) and solution turbidity (red). Error bars represent 95% CI for ELISA and ±1 *SD* for turbidity based on experimental reproducibility results. ELISA, enzyme-linked immunosorbent assay; RABV-G, rabies virus glycoprotein G; *SD*, standard deviation; UVA, ultraviolet radiation; VIS, visible light

(Figure S4). For HEPES/trehalose-based formulations, antigenicity recovery and $T_{unf.III}$ were both improved by pH and reached more than 60% and 58°C, respectively at pH 8 (Figure S4). Nevertheless, an increase of the sodium chloride concentration induced significant negative impact on Tg′ temperature that reached −37°C at pH 8 (Figure S4). Overall, according to statistical results, RABV-G/A8-35 formulated in HEPES/trehalose buffer (F11–F20) showed better stability attributes than those formulated in Tris/trehalose buffer (F1–F10), especially in terms of $T_{unf.III}$ and antigenicity recovery, for which the maximum was predicted at 48% in Tris/trehalose formulation (pH 8.5, sodium chloride 5 g/L) compared with 62% in HEPES/trehalose formulation (pH 8, sodium chloride 3 g/L, Figure 3).

Based on the combination of both high antigenicity recovery and high $T_{unf.III}$, the best formulation for RABV-G/A8-35 was identified as HEPES buffer pH 8, sodium chloride 3 g/L (51.4 mM). This formulation showed a Tg′ at −35°C which is compatible with classical lyophilization process, without additional turbidity of the solution (Figure S4). From the optimized formulation in HEPES buffer, freeze-dried products of RABV-G/A8-35 were prepared with the following characteristics: a residual moisture content of 1.3% and a high glass transition temperature (Tg = 106°C). After re-solubilization of the solid product with water, the RABV-G/A8-35 solution was clear and the antigenic titer was determined at 495 UI/ml. Compared to the initial titer measured before lyophilization (601 UI/ml), a loss of RABV-G antigenicity was assessed to 17 ± 12% during the freeze-dried/re-solubilization process.

RABV-G/A8-35 antigenicity of this freeze-dried formulation remained stable over 2 years at 5°C, 25°C, and 37°C (Figure 4). Regardless of the incubation temperature, no significant loss of RABV-G/A8-35 antigenicity was observed, demonstrating high thermal stability of lyophilized RABV-G/A8-35 complex.

4 | DISCUSSION

The present study investigated the antigenic stability of a viral full-length MP, the rabies virus surface glycoprotein, once extracted with CHAPS and subsequently transferred in APol A8-35 (RABV-G/A8-35). The results demonstrated that the purified RABV-G/A8-35 was folded and antigenically stable. While the thermal stability of RABV-G/A8-35 was enhanced compared with CHAPS, the stability of RABV-G/A8-35 was significantly improved when the complexes were stored under a freeze-dried form compared to a liquid formulation. The freeze-dried form of RABV-G/A8-35 exhibited strong stability for at least 2 years when stored at 5°C and up to 37°C.

To better preserve the protein features and native-like structures, especially in the case of moving antigens, direct extraction of the antigen from the pathogen surface using an accelerated process was considered. This process was performed following three main steps, which are (i) extraction of the full-length G protein from the whole virus by using CHAPS as a mild zwitterionic detergent (Yves Gaudin et al., 1992), (ii) purification of the G protein by sucrose gradient, and then (iii) transfer of the detergent-solubilized G protein to APols using polystyrene beads (Le Bon et al., 2018; Zoonens et al., 2005).

When complexed to APols, MPs are generally more stable than their detergent-solubilized counterpart, as already described for both α-helical MPs like G protein-coupled receptors (Dahmane

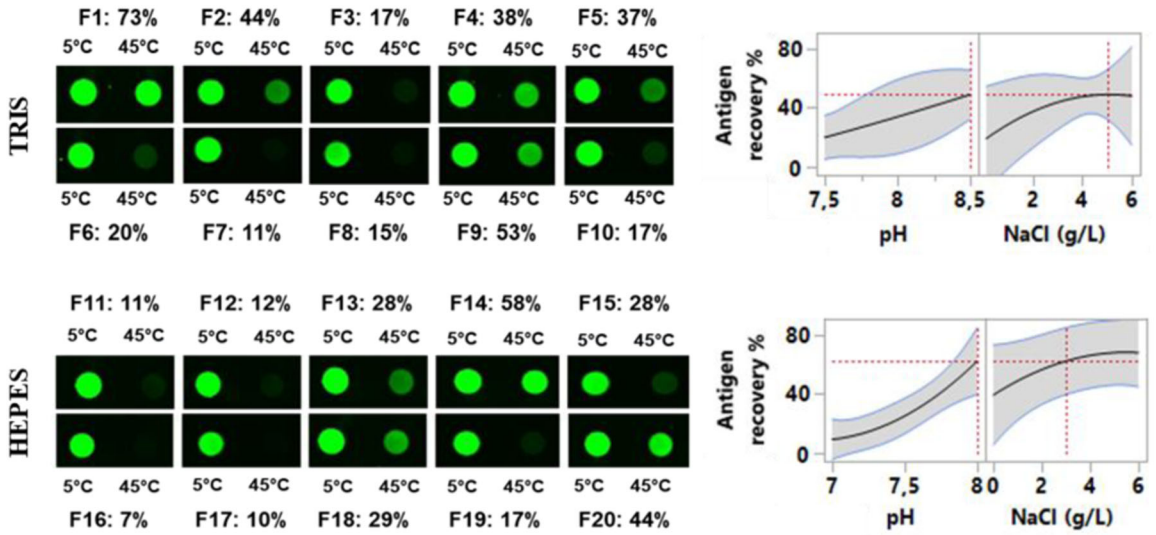

FIGURE 3 Screening of pH-buffer and salt concentration. G-specific dot blots (left) of RABV-G/A8-35 formulations in Tris (top, F1–F10) and HEPES (bottom, F11–F20) buffers after incubation of solutions for 2 days at 5°C and 45°C are presented. Antigenicity recoveries of all formulations (from F1 to F20) are indicated in % as ratio of values at 45°C and 5°C. Prediction profilers (right) for pH and sodium chloride (g/L) were generated from statistical data analysis in JMP. Gray areas depict confidence intervals (95% CI) predictions. The dotted lines indicate the optimized formulation composition considering a set of parameters (antigenicity, Tunf, Tg′, and turbidity, see Figure S4). HEPES, (4-(2-hydroxyethyl)piperazine-1-ethanesulfonic acid, *N*-(2-hydroxyethyl)piperazine-*N*′-(2-ethanesulfonic acid); RABV-G, rabies virus glycoprotein G; Tris, Tris(hydroxymethyl)aminomethane)

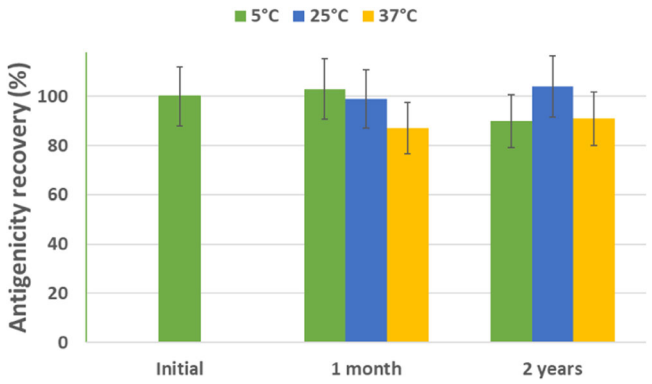

FIGURE 4 Antigenic stability of RABV-G/A8-35 recovered after storage of the protein under a freeze-dried product from 1 month and 2 years at 5°C, (green), 25°C (blue), and 37°C (orange). Antigenicity recoveries determined in % were normalized to the initial value ($t = 0$). Error bars represent 95% CI. CI, confidence interval; RABV-G, rabies virus glycoprotein G

et al., 2009), and β-barrel MPs like the outer membrane protein A (OmpA) from *E. coli* (Pocanschi et al., 2013) or the native major outer membrane protein (nMOMP) purified from lived *Chlamydia* infected-cells (Tifrea et al., 2011). Unsurprisingly, APol A8-35 also improved the stability of the viral bitopic MP RABV-G.

Once purified in CHAPS and detergent exchanged for APol A8-35, RABV-G secondary structure remained unchanged with a mix of α-helices and β-sheets, whose content is in agreement with previously published structures (Fernando et al., 2016). Furthermore, the G-specific antigenicity responses observed before and after surfactant exchange, that is, for RABV-G/CHAPS and RABV-G/A8-35, were both similar to native G glycoprotein found on RABV particle surface, suggesting that the CHAPS solubilization and surfactant exchange processes did not impact the antigen tertiary structure. Using APols can be a simple means of circumventing truncation of transmembrane domain, often used to maintain the solubility of MPs, but requiring time for molecular engineering and protein production processes. This could be of major interest, knowing that truncated MPs can adopt a folded, stable structure different to a certain extent from the ectodomain structure in the complete MPs (Godet et al., 1991; Singh et al., 1990; Vanlandschoot et al., 1996). In the case of RABV-G, membrane anchorage of the protein through the transmembrane domain is involved in the correct folding of the G ectodomain, implying that the transmembrane domain is required to obtain the ectodomain native form (Y. Gaudin et al., 1999; Maillard & Gaudin, 2002). Previous studies reported that APols spontaneously form a belt surrounding the transmembrane region of the protein and, if available, protein-bound lipids (Popot, 2018). Regarding the glycosylation sites, which are located far from the transmembrane domain, they should remain accessible in RABV-G/A8-35.

The temperatures of protein denaturation determined by nDSF were around 6°C higher in A8-35 compared to the CHAPS condition (Table 1). Interestingly, losses of antigenicity predicted by kinetic models were in agreement with loss of tertiary structure experimentally observed by nDSF, showing a gap of approximately +5°C between the two formulations (Figure S3). This strengthens the confidence in the kinetic models and opens up a wide field of applications of protein stability predictions (Clénet, 2018; Roduit et al., 2019). Based on a kinetic modeling approach, it was predicted that RABV-G/A8-35 samples should be stable at least for 1 year at 5°C, whereas RABV-G/CHAPS samples could lose more than 50% of antigenicity under the same storage conditions, confirming the stabilizing effect of A8-35 as observed experimentally during one month at 5°C and 25°C (Figure 1). Moreover, the thermal stability of G-specific antigenicity from the whole RABV virus (Clenet et al., 2018) and after trapping into A8-35 seemed to be similar. Regarding other antigenic MPs, the nMOMP from *C. muridarum* was antigenically more stable in A8-35 (for at least 100 days at room temperature) than in zwittergent Z3-14 (Feinstein et al., 2014). Many other studies have reported that APol A8-35 significantly increases the lifetime of MPs (Popot, 2018). Together, these results suggest that the stability of protein formulations is heightened by A8-35 regardless of the MP topology. Additionally, A8-35 mixed with dodecylmaltoside (DDM) has recently helped to solve the crystal structure of the full-length glycoprotein B from Herpes virus (Cooper et al., 2018), which adopts a trimeric arrangement like RABV-G. Furthermore, the structure of the full-length trimeric HIV-1 envelope glycoprotein was obtained in a mixture of APol A8-35 and cyclohexyl-hexyl-β-D-maltosid (CYMAL-6) glycosidic surfactant with single-particle electron cryo-microscopy (Zhang et al., 2018).

From a pharmaceutical production point of view, different types of stresses on bioproducts can occur before usage, affecting the product integrity. For instance, temperature excursions, light exposure, and agitation through shaking during transport are of major concern. Thus, to determine the magnitude of the damage which RABV-G solutions may undergo under such conditions, light exposure as well as mechanical stress were tested in parallel to the RABV-G thermal stability characterization. Evaluation of the effect of these stresses is commonly performed during formulation development of vaccines with the aim of identifying the main degradation pathways (Ausar et al., 2013). This allows one to anticipate impact of postproduction handling and unintentional mishandling of bioproducts (Grabarek et al., 2020; Nejadnik et al., 2018). As recommended by international conference harmonization (ICH) Q1B guidelines (ICH Topic Q1B—Photostability Testing of New Active Substances and Medicinal Products, 1998) about photostability testing of drug substances and products, photolytic susceptibility of proteins has to be estimated using light providing an overall illumination of not less than 1.2 million lux·hour and an integrated near ultraviolet energy of not less than 200 W h/m^2. It was pointed out that these conditions specified in ICHQ1B were first implemented for active pharmaceutical ingredients and may not be appropriate for all proteins because it may be too destructive (EBE, 2015). The loss of 50% of G-specific antigenicity after ICH high-level light exposures of RABV-G/A8-35 solution exemplified the photodegradation of G protein (Figure 2). Considered as forced degradation testing studies, more moderated light exposure conditions have been recommended as "confirmatory

testing studies" to predict the stability of the product. For instance, some authors adjusted light exposure at 50% of ICH recommended light exposure for a photosensitive enveloped attenuated virus (Ausar et al., 2013). Generally, the exposure of protein solutions to ICH light conditions led to the generation of aggregates (Kerwin & Remmele, 2007; Sreedhara et al., 2016). In the case of RABV-G/A8-35 solution, the turbidity remained unchanged under light stress, suggesting that G protein lost its antigenicity under light exposure through mechanisms other than aggregation.

Agitation was used to evaluate RABV-G/A8-35 sensitivity during handling, transportation and unintentional mishandling of vials. Under agitation stress conditions (stirring), a loss of G-specific antigenicity of RABV-G was progressively observed as a function of time with a concomitant increase of turbidity indicating emergence of protein aggregates in solution (Figure 2). Among mechanical stress conditions, it has been shown that stirring is one of the more stressful, leading to aggregation of proteins and/or flocculation and a significant increasing of turbidity of solutions (Gandhi et al., 2017; Ghazvini et al., 2016; Kiese et al., 2008; Koepf et al., 2018; Schack et al., 2018). This suggests that vaccine subunit antigen such as RABV-G may be sensitive to stirring in the same way that monoclonal antibodies in solution, hence requiring stabilization efforts. This major physical instability exhibited by proteins in solution could also promote inappropriate biological responses and unwanted immunogenicity related to aggregates present in protein-based pharmaceuticals (Freitag et al., 2015; Schellekens, 2005).

For many proteins, which are sensitive to mechanical agitation in solution, solid forms can be an appropriate alternative, especially for transportation issues and long-term storage of products (several years at 5°C). Freeze-dried, spray-dried, or foam-dried products, as well as micro-needles and potentially freeze-dried micropellets are examples of solid forms of biotherapeutics and vaccines (Abdul-Fattah et al., 2007; Clenet et al., 2019; Ohtake et al., 2010). Among them, freeze-drying process is regularly used to maintain the stability of bioproducts in a solid-state for years under refrigerated storage conditions (Gervasi et al., 2018; Hansen et al., 2015). The formulation composition of RABV-G/A8-35 complex was optimized for freeze-drying process, first by adding trehalose as a lyoprotectant, bulking agent and glass transition enhancer (Jain & Roy, 2009; Starciuc et al., 2020) and second, through screening pH and ionic strength using designs of experiments. The solubility of A8-35 is conferred by the carboxylate groups, which are ionized above neutral pH, but begin to protonate at pH below 7.0, resulting in polymer precipitation (Gohon et al., 2006). In the present study, pH ranges varying from 7.0 to 8.5 were tested in formulations using either Tris or HEPES buffers, while the ionic strength of RABV-G/A8-35 formulations was managed by adding sodium chloride at concentrations ranging from 5 to 103 mM. Our study demonstrated that HEPES buffer was more effective than Tris buffer. RABV-G/A8-35 formulated in 20 mM HEPES (pH 8.0) with trehalose (292 mM) and sodium chloride (50 mM) resulted in the highest recovery of G-specific antigenicity (Figure 3), unfolding temperature enhancement and resistance to aggregation (Figure S4). To our knowledge, this is the first report of a G-specific antigenic RABV-G/A8-35 freeze-dried product shown to be experimentally highly stable for 2 years at 5°C, 25°C and 37°C (Figure 4). The highest incubation temperature (i.e., 37°C) was far below the glass transition temperature of the product (Tg = 106°C). As a result, at 37°C, RABV-G was still under a glassy state which strongly blocks cooperative molecular mobility and potential associated instabilities. It is commonly assumed that the storage temperature should be at least 20° below the glass transition temperature (Carpenter et al., 1997). This certainly contributes to explain the long-term stability and low thermal sensitivity of this freeze-dried product, suggesting that storage of RABV-G/A8-35 freeze-dried product at ambient temperature could be considered. This could be of high interest for bioproducts such as vaccines, which can be exposed to elevated ambient temperatures (e.g., few days at around 40°C) during the latter stages of transportation, especially in endemic zones in Sub-Saharan Africa and South America (Kartoglu & Milstien, 2014). Previous studies demonstrated the ability of polymers like Dextran, carboxymethyl cellulose and polyethylene glycol to prevent protein deterioration during lyophilization and after freeze-dried product rehydration (Costantino et al., 1995; Liu et al., 1991). Based on the results presented here, A8-35 showed its compatibility with freeze-drying process and can also join the list of polymers that have demonstrated a stabilizing effect for proteins stored in solid form.

The biodistribution and elimination rate of A8-35 when injected in mice via three different delivery routes (intravenous, intraperitoneal, and subcutaneous) was characterized using a fluorescent version of A8-35 (Fernandez et al., 2014). The absence of APol toxicity was also demonstrated by the absence of antibody response raised against APols (Popot et al., 2003). Previous studies showed immunogenicity results in a murine model using trimeric beta-barrel MOMP purified from *C. muridarum*, with improved protection observed when the detergent was exchanged for plain or adjuvant-functionalized A8-35 (Tifrea et al., 2011, 2014, 2018, 2020). Since full-length RABV-G was solubilized and stabilized in an A8-35 containing formulation, as illustrated by the results presented herein, the level of protection in vaccinated mice will deserve further investigations.

5 | CONCLUSION

The present study reports the improved stability of full-length G protein from rabies virus in the presence of A8-35, confirming the ability of APols to stabilize pathogen surface MPs. RABV-G/A8-35 exhibited high thermal stability of G-specific antigenicity in a defined freeze-dried formulation for at least 2 years under storage conditions from 5°C to 37°C. Finally, to the best of our knowledge, this is the first demonstration of long-term antigenic stability of natural full-length MP directly extracted from a virus, and then complexed to APols. These results describe a simple process implemented to obtain the antigen of interest, purified and stabilized under its native-like conformation, directly from a pathogen (reference or circulating strains), which is of high interest for diagnosis (quantification/characterizations assays), therapeutic and vaccine strategies. Following

this protein physical characterization, identification of RABV-G/A8-35 neutralizing epitopes is underway before conducting in vivo evaluation.

ACKNOWLEDGMENTS

The authors would like to express their sincere thanks to Hubert Venet for his technical contribution for protein extraction, purification, and formulation processes; Fabien Guinchard for ELISA analyses under the supervision of Vanessa Boulay; Alexey Rak and Saskia Villinger for nano-DSF experiments, Frédéric Gréco for circular dichroism experiments and Ziad Harmouche who initiated the use of Amphipols in the Sanofi group. In addition, the amphipol development in IBPC Paris was supported by the Centre National de la Recherche Scientifique (CNRS), Université de Paris (Université Paris 7), and the "Initiative d'Excellence" program from the French State (Grant "DYNAMO," ANR-11-LABX-0011-01).

CONFLICT OF INTERESTS

Didier Clénet and Aure Saulnier are employees of Sanofi Pasteur. Léna Clavier and Benoît Strobbe were trainees at Sanofi-Pasteur. Christel Le Bon and Manuela Zoonens are CNRS employees.

AUTHOR CONTRIBUTIONS

Didier Clénet and Aure Saulnier conceived and designed the project, performed experiments, analyzed the data, and co-wrote the article. Léna Clavier and Benoît Strobbe performed experiments, data analysis, and co-wrote the article. Christel Le Bon and Manuela Zoonens trained Sanofi-Pasteur on the use of Amphipols, shared technical advice, and co-wrote the article.

DATA AVAILABILITY STATEMENT

The data that support the findings of this study are available on request from the corresponding author. The data are not publicly available due to privacy or ethical restrictions.

ORCID

Didier Clénet http://orcid.org/0000-0002-8395-9430
Manuela Zoonens https://orcid.org/0000-0003-2648-7868

REFERENCES

Abdul-Fattah, A. M., Truong-Le, V., Yee, L., Pan, E., Ao, Y., Kalonia, D. S., & Pikal, M. J. (2007). Drying-induced variations in physico-chemical properties of amorphous pharmaceuticals and their impact on Stability II: Stability of a vaccine. *Pharmaceutical Research*, *24*(4), 715–727. https://doi.org/10.1007/s11095-006-9191-2

Albertini, A. A., Baquero, E., Ferlin, A., & Gaudin, Y. (2012). Molecular and cellular aspects of rhabdovirus entry. *Viruses*, *4*(1), 117–139. https://doi.org/10.3390/v4010117

Alberts B, J. A., & Lewis, J., et al (2002). *Membrane proteins can be solubilized and purified in detergents. in molecular biology of the cell* (4th ed.). Garland Science.

Ausar, S. F., Hasija, M., Li, L., & Rahman, N. (2013). Forced degradation studies: an essential tool for the formulation development of vaccines. *Vaccine: Development and Therapy*, *3*, 11–33. https://doi.org/10.2147/vdt.S41998

Belot, L., Albertini, A., & Gaudin, Y. (2019). Chapter five: Structural and cellular biology of rhabdovirus entry. In M. Kielian, T. C. Mettenleiter, & M. J. Roossinck (Eds.), *Advances in virus research* (Vol. 104, pp. 147–183). Academic Press.

Blesneac, I., Ravaud, S., Juillan-Binard, C., Barret, L. A., Zoonens, M., Polidori, A., Miroux, B., Pucci, B., & Pebay-Peyroula, E. (2012). Production of UCP1 a membrane protein from the inner mitochondrial membrane using the cell free expression system in the presence of a fluorinated surfactant. *Biochimica et Biophysica Acta/General Subjects*, *1818*(3), 798–805. https://doi.org/10.1016/j.bbamem.2011.12.016

Carpenter, J. F., Pikal, M. J., Chang, B. S., & Randolph, T. W. (1997). Rational design of stable lyophilized protein formulations: Some practical advice. *Pharmaceutical Research*, *14*(8), 969–975. https://doi.org/10.1023/a:1012180707283

Chabaud-Riou, M., Moreno, N., Guinchard, F., Nicolai, M. C., Niogret-Siohan, E., Sève, N., Manin, C., Guinet-Morlot, F., & Riou, P. (2017). G-protein based ELISA as a potency test for rabies vaccines. *Biologicals*, *46*, 124–129. https://doi.org/10.1016/j.biologicals.2017.02.002

Charvolin, D., Perez, J. B., Rouvière, F., Giusti, F., Bazzacco, P., Abdine, A., Rappaport, F., Martinez, K. L., & Popot, J. L. (2009). The use of amphipols as universal molecular adapters to immobilize membrane proteins onto solid supports. *Proceedings of the National Academy of Sciences of the United States of America*, *106*(2), 405–410. https://doi.org/10.1073/pnas.0807132106

Ci, Y., Yang, Y., Xu, C., & Shi, L. (2018). Vesicular stomatitis virus G protein transmembrane region is crucial for the hemi-fusion to full fusion transition. *Scientific Reports*, *8*(1), 10669. https://doi.org/10.1038/s41598-018-28868-y

Clénet, D. (2018). Accurate prediction of vaccine stability under real storage conditions and during temperature excursions. *European Journal of Pharmaceutics and Biopharmaceutics*, *125*, 76–84. https://doi.org/10.1016/j.ejpb.2018.01.005

Clénet, D., Hourquet, V., Woinet, B., Ponceblanc, H., & Vangelisti, M. (2019). A spray freeze dried micropellet based formulation proof-of-concept for a yellow fever vaccine candidate. *European Journal of Pharmaceutics and Biopharmaceutics*, *142*, 334–343. https://doi.org/10.1016/j.ejpb.2019.07.008

Clénet, D., Vinit, T., Soulet, D., Maillet, C., Guinet-Morlot, F., & Saulnier, A. (2018). Biophysical virus particle specific characterization to sharpen the definition of virus stability. *European Journal of Pharmaceutics and Biopharmaceutics*, *132*, 62–69. https://doi.org/10.1016/j.ejpb.2018.08.006

Cooper, R. S., Georgieva, E. R., Borbat, P. P., Freed, J. H., & Heldwein, E. E. (2018). Structural basis for membrane anchoring and fusion regulation of the herpes simplex virus fusogen gB. *Nature Structural & Molecular Biology*, *25*(5), 416–424. https://doi.org/10.1038/s41594-018-0060-6

Costantino, H. R., Langer, R., & Klibanov, A. M. (1995). Aggregation of a lyophilized pharmaceutical protein, recombinant human albumin: Effect of moisture and stabilization by excipients. *Biotechnology*, *13*(5), 493–496. https://doi.org/10.1038/nbt0595-493

Dahmane, T., Damian, M., Mary, S., Popot, J. L., & Baneres, J. L. (2009). Amphipol-assisted in vitro folding of G protein-coupled receptors. *Biochemistry*, *48*(27), 6516–6521. https://doi.org/10.1021/bi801729z

Della Pia, E. A., Hansen, R. W., Zoonens, M., & Martinez, K. L. (2014). Functionalized amphipols: A versatile toolbox suitable for applications of membrane proteins in synthetic biology. *The Journal of Membrane Biology*, *247*(9), 815–826. https://doi.org/10.1007/s00232-014-9663-y

Della Pia, E. A., Holm, J. V., Lloret, N., Le Bon, C., Popot, J. L., Zoonens, M., Nygård, J., & Martinez, K. L. (2014). A step closer to membrane

protein multiplexed nanoarrays using biotin-doped polypyrrole. *ACS Nano*, *8*(2), 1844–1853. https://doi.org/10.1021/nn406252h

Dilworth, M. V., Piel, M. S., Bettaney, K. E., Ma, P., Luo, J., Sharples, D., Poyner, D. R., Gross, S. R., Moncoq, K., Henderson, P., Miroux, B., & Bill, R. M. (2018). Microbial expression systems for membrane proteins. *Methods*, *147*, 3–39. https://doi.org/10.1016/j.ymeth.2018.04.009

Dorr, J. M., Scheidelaar, S., Koorengevel, M. C., Dominguez, J. J., Schafer, M., van Walree, C. A., & Killian, J. A. (2016). The styrene-maleic acid copolymer: A versatile tool in membrane research. *European Biophysics Journal*, *45*(1), 3–21. https://doi.org/10.1007/s00249-015-1093-y

Duquesne, K., & Sturgis, J. N. (2010). Membrane protein solubilization. In I. Mus-Veteau (Ed.), *Heterologous expression of membrane proteins: Methods and protocols* (pp. 205–217). Humana Press.

EBE. (2015). Forced degradation studies for therapeutic proteins. European Biopharmaceutical Enterprises, concept paper.

Feinstein, H. E., Tifrea, D., Sun, G., Popot, J. L., de la Maza, L. M., & Cocco, M. J. (2014). Long-term stability of a vaccine formulated with the amphipol-trapped major outer membrane protein from Chlamydia trachomatis. *The Journal of Membrane Biology*, *247*(9-10), 1053–1065. https://doi.org/10.1007/s00232-014-9693-5

Fernandez, A., Le Bon, C., Baumlin, N., Giusti, F., Cremel, G., Popot, J. L., & Bagnard, D. (2014). In vivo characterization of the biodistribution profile of amphipol A8-35. *The Journal of Membrane Biology*, *247*(9-10), 1043–1051. https://doi.org/10.1007/s00232-014-9682-8

Fernando, B. G., Yersin, C. T., Jose, C. B., & Paola, Z. S. (2016). Predicted 3D model of the rabies virus glycoprotein trimer. *BioMed Research International*, *2016*, 1674580. https://doi.org/10.1155/2016/1674580

Freitag, A. J., Shomali, M., Michalakis, S., Biel, M., Siedler, M., Kaymakcalan, Z., Carpenter, J. F., Randolph, T. W., Winter, G., & Engert, J. (2015). Investigation of the immunogenicity of different types of aggregates of a murine monoclonal antibody in mice. *Pharmaceutical Research*, *32*(2), 430–444. https://doi.org/10.1007/s11095-014-1472-6

Gandhi, A. V., Pothecary, M. R., Bain, D. L., & Carpenter, J. F. (2017). Some lessons learned from a comparison between sedimentation velocity analytical ultracentrifugation and size exclusion chromatography to characterize and quantify protein aggregates. *Journal of Pharmaceutical Sciences*, *106*(8), 2178–2186. https://doi.org/10.1016/j.xphs.2017.04.048

Gaudin, Y., Moreira, S., J, B. N. J., Blondel, D., Flamand, A., & Tuffereau, C. (1999). Soluble ectodomain of rabies virus glycoprotein expressed in eukaryotic cells folds in a monomeric conformation that is antigenically distinct from the native state of the complete, membrane-anchored glycoprotein. *Journal of General Virology*, *80 (Pt 7)*(7), 1647–1656. https://doi.org/10.1099/0022-1317-80-7-1647

Gaudin, Y., Ruigrok, R. W. H., Tuffereau, C., Knossow, M., & Flamand, A. (1992). Rabies virus glycoprotein is a trimer. *Virology*, *187*(2), 627–632. https://doi.org/10.1016/0042-6822(92)90465-2

Gervasi, V., Dall Agnol, R., Cullen, S., McCoy, T., Vucen, S., & Crean, A. (2018). Parenteral protein formulations: An overview of approved products within the European Union. *European Journal of Pharmaceutics and Biopharmaceutics*, *131*, 8–24. https://doi.org/10.1016/j.ejpb.2018.07.011

Ghazvini, S., Kalonia, C., Volkin, D. B., & Dhar, P. (2016). Evaluating the role of the air-solution interface on the mechanism of subvisible particle formation caused by mechanical agitation for an IgG1 mAb. *Journal of Pharmaceutical Sciences*, *105*(5), 1643–1656. https://doi.org/10.1016/j.xphs.2016.02.027

Giusti, F., Kessler, P., Hansen, R. W., Della Pia, E. A., Le Bon, C., Mourier, G., Popot, J. L., Martinez, K. L., & Zoonens, M. (2015). Synthesis of a polyhistidine-bearing amphipol and its use for immobilizing membrane proteins. *Biomacromolecules*, *16*(12), 3751–3761. https://doi.org/10.1021/acs.biomac.5b01010

Godet, M., Rasschaert, D., & Laude, H. (1991). Processing and antigenicity of entire and anchor-free spike glycoprotein S of coronavirus TGEV expressed by recombinant baculovirus. *Virology*, *185*(2), 732–740. https://doi.org/10.1016/0042-6822(91)90544-I

Gohon, Y., Giusti, F., Prata, C., Charvolin, D., Timmins, P., Ebel, C., Tribet, C., & Popot, J. L. (2006). Well-defined nanoparticles formed by hydrophobic assembly of a short and polydisperse random terpolymer, amphipol A8-35. *Langmuir*, *22*(3), 1281–1290. https://doi.org/10.1021/la052243g

Grabarek, A. D., Bozic, U., Rousel, J., Menzen, T., Kranz, W., Wuchner, K., Jiskoot, W., & Hawe, A. (2020). What makes polysorbate functional? Impact of polysorbate 80 grade and quality on IgG stability during mechanical stress. *Journal of Pharmaceutical Sciences*, *109*(1), 871–880. https://doi.org/10.1016/j.xphs.2019.10.015

Hansen, L. J. J., Daoussi, R., Vervaet, C., Remon, J. P., & De Beer, T. R. M. (2015). Freeze-drying of live virus vaccines: A review. *Vaccine*, *33*(42), 5507–5519. https://doi.org/10.1016/j.vaccine.2015.08.085

Hardy, D., Bill, R. M., Jawhari, A., & Rothnie, A. J. (2016). Overcoming bottlenecks in the membrane protein structural biology pipeline. *Biochemical Society Transactions*, *44*(3), 838–844. https://doi.org/10.1042/BST20160049

Hardy, D., Bill, R. M., Rothnie, A. J., & Jawhari, A. (2019). Stabilization of human multidrug resistance protein 4 (MRP4/ABCC4) using novel solubilization agents. *SLAS Discovery*, *24*(10), 1009–1017. https://doi.org/10.1177/2472555219867074

ICH Topic Q1B: Photostability testing of new active substances and medicinal products. (1998).

Ionescu-Matiu, I., Kennedy, R. C., Sparrow, J. T., Culwell, A. R., Sanchez, Y., Melnick, J. L., & Dreesman, G. R. (1983). Epitopes associated with a synthetic hepatitis B surface antigen peptide. *Journal of Immunology*, *130*(4), 1947–1952.

Jain, N. K., & Roy, I. (2009). Effect of trehalose on protein structure. *Protein Science*, *18*(1), 24–36. https://doi.org/10.1002/pro.3

Kartoglu, U., & Milstien, J. (2014). Tools and approaches to ensure quality of vaccines throughout the cold chain. *Expert Review of Vaccines*, *13*(7), 843–854. https://doi.org/10.1586/14760584.2014.923761

Kerwin, B. A., & Remmele, R. L. Jr. (2007). Protect from light: Photodegradation and protein biologics. *Journal of Pharmaceutical Sciences*, *96*(6), 1468–1479. https://doi.org/10.1002/jps.20815

Kiese, S., Papppenberger, A., Friess, W., & Mahler, H. C. (2008). Shaken, not stirred: Mechanical stress testing of an IgG1 antibody. *Journal of Pharmaceutical Sciences*, *97*(10), 4347–4366. https://doi.org/10.1002/jps.21328

Knowles, T. J., Finka, R., Smith, C., Lin, Y. P., Dafforn, T., & Overduin, M. (2009). Membrane proteins solubilized intact in lipid containing nanoparticles bounded by styrene maleic acid copolymer. *Journal of the American Chemical Society*, *131*(22), 7484–7485. https://doi.org/10.1021/ja810046q

Koepf, E., Schroeder, R., Brezesinski, G., & Friess, W. (2018). The missing piece in the puzzle: Prediction of aggregation via the protein-protein interaction parameter A(*)2. *European Journal of Pharmaceutics and Biopharmaceutics*, *128*, 200–209. https://doi.org/10.1016/j.ejpb.2018.04.024

Le Bon, C., Della Pia, E. A., Giusti, F., Lloret, N., Zoonens, M., Martinez, K. L., & Popot, J. L. (2014). Synthesis of an oligonucleotide-derivatized amphipol and its use to trap and immobilize membrane proteins. *Nucleic Acids Research*, *42*(10), e83. https://doi.org/10.1093/nar/gku250

Le Bon, C., Marconnet, A., Masscheleyn, S., Popot, J. L., & Zoonens, M. (2018). Folding and stabilizing membrane proteins in amphipol A8-35. *Methods*, *147*, 95–105. https://doi.org/10.1016/j.ymeth.2018.04.012

Liu, W. R., Langer, R., & Klibanov, A. M. (1991). Moisture-induced aggregation of lyophilized proteins in the solid state. *Biotechnology and Bioengineering*, *37*(2), 177–184. https://doi.org/10.1002/bit.260370210

Maillard, A. P., & Gaudin, Y. (2002). Rabies virus glycoprotein can fold in two alternative, antigenically distinct conformations depending on membrane-anchor type. *Journal of General Virology*, *83*(Pt 6), 1465–1476. https://doi.org/10.1099/0022-1317-83-6-1465

Mandon, E. D., Pizzorno, A., Traversier, A., Champagne, A., Hamelin, M. E., Lina, B., Boivin, G., Dejean, E., Rosa-Calatrava, M., & Jawhari, A. (2020). Novel calixarene-based surfactant enables low dose split inactivated vaccine protection against influenza infection. *Vaccine*, *38*(2), 278–287. https://doi.org/10.1016/j.vaccine.2019.10.018

Marconnet, A., Michon, B., Le Bon, C., Giusti, F., Tribet, C., & Zoonens, M. (2020). Solubilization and stabilization of membrane proteins by cycloalkane-modified amphiphilic polymers. *Biomacromolecules*, *21*(8), 3459–3467. https://doi.org/10.1021/acs.biomac.0c00929

Matar-Merheb, R., Rhimi, M., Leydier, A., Huché, F., Galián, C., Desuzinges-Mandon, E., Ficheux, D., Flot, D., Aghajari, N., Kahn, R., Di Pietro, A., Jault, J. M., Coleman, A. W., & Falson, P. (2011). Structuring detergents for extracting and stabilizing functional membrane proteins. *PLoS One*, *6*(3), e18036. https://doi.org/10.1371/journal.pone.0018036

Nejadnik, M. R., Randolph, T. W., Volkin, D. B., Schöneich, C., Carpenter, J. F., Crommelin, D. J. A., & Jiskoot, W. (2018). Postproduction handling and administration of protein pharmaceuticals and potential instability issues. *Journal of Pharmaceutical Sciences*, *107*(8), 2013–2019. https://doi.org/10.1016/j.xphs.2018.04.005

Ohtake, S., Martin, R. A., Yee, L., Chen, D., Kristensen, D. D., Lechuga-Ballesteros, D., & Truong-Le, V. (2010). Heat-stable measles vaccine produced by spray drying. *Vaccine*, *28*(5), 1275–1284. https://doi.org/10.1016/j.vaccine.2009.11.024

Orwick-Rydmark, M., Arnold, T., & Linke, D. (2016). The use of detergents to purify membrane proteins. *Current Protocols in Protein Science*, *84*(1), 481–485. https://doi.org/10.1002/0471140864.ps0408s84

Otzen, D. E. (2015). Proteins in a brave new surfactant world. *Current Opinion in Colloid & Interface Science*, *20*(3), 161–169. https://doi.org/10.1016/j.cocis.2015.07.003

Pocanschi, C. L., Popot, J. L., & Kleinschmidt, J. H. (2013). Folding and stability of outer membrane protein A (OmpA) from *Escherichia coli* in an amphipathic polymer, amphipol A8-35. *European Biophysics Journal*, *42*(2-3), 103–118. https://doi.org/10.1007/s00249-013-0887-z

Popot, J. L. (2010). Amphipols, nanodiscs, and fluorinated surfactants: Three nonconventional approaches to studying membrane proteins in aqueous solutions. *Annual Review of Biochemistry*, *79*(1), 737–775. https://doi.org/10.1146/annurev.biochem.052208.114057

Popot, J. L. (2018). Membrane proteins in aqueous solutions: From detergents to amphipols, *Biological and medical physics, biomedical engineering*. Springer. https://doi.org/10.1007/978-3-319-73148-3

Popot, J. L., Althoff, T., Bagnard, D., Banères, J. L., Bazzacco, P., Billon-Denis, E., Catoire, L. J., Champeil, P., Charvolin, D., Cocco, M. J., Crémel, G., Dahmane, T., de la Maza, L. M., Ebel, C., Gabel, F., Giusti, F., Gohon, Y., Goormaghtigh, E., Guittet, E., … Zoonens, M. (2011). Amphipols from A to Z. *Annual Review of Biophysics*, *40*(1), 379–408. https://doi.org/10.1146/annurev-biophys-042910-155219

Popot, J. L., Berry, E. A., Charvolin, D., Creuzenet, C., Ebel, C., Engelman, D. M., Flötenmeyer, M., Giusti, F., Gohon, Y., Hong, Q., Lakey, J. H., Leonard, K., Shuman, H. A., Timmins, P., Warschawski, D. E., Zito, F., Zoonens, M., Pucci, B., & Tribet, C. (2003). Amphipols: Polymeric surfactants for membrane biology research. *Cellular and Molecular Life Science*, *60*(8), 1559–1574. https://doi.org/10.1007/s00018-003-3169-6

Qoronfleh, M. W., Hesterberg, L. K., & Seefeldt, M. B. (2007). Confronting high-throughput protein refolding using high pressure and solution screens. *Protein Expression and Purification*, *55*(2), 209–224. https://doi.org/10.1016/j.pep.2007.05.014

Roduit, B., Hartmann, M., Folly, P., Sarbach, A., & Baltensperger, R. (2014). Prediction of thermal stability of materials by modified kinetic and model selection approaches based on limited amount of experimental points. *Thermochimica Acta*, *579*, 31–39. https://doi.org/10.1016/j.tca.2014.01.005

Roduit, B., Luyet, C. A., Hartmann, M., Folly, P., Sarbach, A., Dejeaifve, A., Dobson, R., Schroeter, N., Vorlet, O., Dabros, M., & Baltensperger, R. (2019). Continuous monitoring of shelf lives of materials by application of data loggers with implemented kinetic parameters. *Molecules*, *24*(12), 2217. https://doi.org/10.3390/molecules24122217

Roque, C., Ausar, S. F., Raham, N., & Clénet, D. (2021). Stability modeling in QbD: Accelerating formulation development and predicting shelf life of products, *Quality by design: An indispensable approach to accelerate biopharmaceutical product development* (pp. 169–199). PDA.

Sadaf, A., Cho, K. H., Byrne, B., & Chae, P. S. (2015). Chapter four: Amphipathic agents for membrane protein study. In A. K. Shukla (Ed.), *Methods in enzymology* (Vol. 557, pp. 57–94). Academic Press.

Schack, M. M., Moller, E. H., Carpenter, J. F., Rades, T., & Groenning, M. (2018). A platform for preparing homogeneous proteinaceous subvisible particles with distinct morphologies. *Journal of Pharmaceutical Sciences*, *107*(7), 1842–1851. https://doi.org/10.1016/j.xphs.2018.03.014

Schellekens, H. (2005). Factors influencing the immunogenicity of therapeutic proteins. *Nephrology, Dialysis, Transplantation*, *20*(suppl_6), Svi3–Svi9. https://doi.org/10.1093/ndt/gfh1092

Simon, K. S., Pollock, N. L., & Lee, S. C. (2018). Membrane protein nanoparticles: The shape of things to come. *Biochemical Society Transactions*, *46*(6), 1495–1504. https://doi.org/10.1042/BST20180139

Singh, I., Doms, R. W., Wagner, K. R., & Helenius, A. (1990). Intracellular transport of soluble and membrane-bound glycoproteins: Folding, assembly and secretion of anchor-free influenza hemagglutinin. *The EMBO Journal*, *9*(3), 631–639.

Smith, E. C., Culler, M. R., Hellman, L. M., Fried, M. G., Creamer, T. P., & Dutch, R. E. (2012). Beyond anchoring: the expanding role of the hendra virus fusion protein transmembrane domain in protein folding, stability, and function. *Journal of Virology*, *86*(6), 3003–3013. https://doi.org/10.1128/JVI.05762-11

Smith, E. C., Smith, S. E., Carter, J. R., Webb, S. R., Gibson, K. M., Hellman, L. M., Fried, M. G., & Dutch, R. E. (2013). Trimeric transmembrane domain interactions in paramyxovirus fusion proteins: roles in protein folding, stability, and function. *The Journal of Biological Chemistry*, *288*(50), 35726–35735. https://doi.org/10.1074/jbc.M113.514554

Sreedhara, A., Yin, J., Joyce, M., Lau, K., Wecksler, A. T., Deperalta, G., Yi, L., John Wang, Y., Kabakoff, B., & Kishore, R. S. (2016). Effect of ambient light on IgG1 monoclonal antibodies during drug product processing and development. *European Journal of Pharmaceutics and Biopharmaceutics*, *100*, 38–46. https://doi.org/10.1016/j.ejpb.2015.12.003

Starciuc, T., Malfait, B., Danede, F., Paccou, L., Guinet, Y., Correia, N. T., & Hedoux, A. (2020). Trehalose or sucrose: Which of the two should be used for stabilizing proteins in the solid state? A dilemma investigated by in situ micro-raman and dielectric relaxation spectroscopies during and after freeze-drying. *Journal of Pharmaceutical Sciences*, *109*(1), 496–504. https://doi.org/10.1016/j.xphs.2019.10.055

Stroud, Z., Hall, S. C. L., & Dafforn, T. R. (2018). Purification of membrane proteins free from conventional detergents: SMA, new polymers,

new opportunities and new insights. *Methods*, *147*, 106–117. https://doi.org/10.1016/j.ymeth.2018.03.011

Suzich, J. A., Ghim, S. J., Palmer-Hill, F. J., White, W. I., Tamura, J. K., Bell, J. A., Newsome, J. A., Jenson, A. B., & Schlegel, R. (1995). Systemic immunization with papillomavirus L1 protein completely prevents the development of viral mucosal papillomas. *Proceedings of the National Academy of Sciences of the United States of America*, *92*(25), 11553–11557. https://doi.org/10.1073/pnas.92.25.11553

Tifrea, D. F., Pal, S., le Bon, C., Cocco, M. J., Zoonens, M., & de la Maza, L. M. (2020). Improved protection against *Chlamydia muridarum* using the native major outer membrane protein trapped in Resiquimod-carrying amphipols and effects in protection with addition of a Th1 (CpG-1826) and a Th2 (Montanide ISA 720) adjuvant. *Vaccine*, *38*, 4412–4422. https://doi.org/10.1016/j.vaccine.2020.04.065

Tifrea, D. F., Pal, S., Le Bon, C., Giusti, F., Popot, J. L., Cocco, M. J., Zoonens, M., & de la Maza, L. M. (2018). Co-delivery of amphipol-conjugated adjuvant with antigen, and adjuvant combinations, enhance immune protection elicited by a membrane protein-based vaccine against a mucosal challenge with Chlamydia. *Vaccine*, *36*(45), 6640–6649. https://doi.org/10.1016/j.vaccine.2018.09.055

Tifrea, D. F., Pal, S., Popot, J. L., Cocco, M. J., & de la Maza, L. M. (2014). Increased immunoaccessibility of MOMP epitopes in a vaccine formulated with amphipols may account for the very robust protection elicited against a vaginal challenge with *Chlamydia muridarum*. *Journal of Immunology*, *192*(11), 5201–5213. https://doi.org/10.4049/jimmunol.1303392

Tifrea, D. F., Sun, G., Pal, S., Zardeneta, G., Cocco, M. J., Popot, J. L., & de la Maza, L. M. (2011). Amphipols stabilize the *Chlamydia* major outer membrane protein and enhance its protective ability as a vaccine. *Vaccine*, *29*(28), 4623–4631. https://doi.org/10.1016/j.vaccine.2011.04.065

Tribet, C., Audebert, R., & Popot, J. L. (1996). Amphipols: Polymers that keep membrane proteins soluble in aqueous solutions. *Proceedings of the National Academy of Sciences of the United States of America*, *93*(26), 15047–15050. https://doi.org/10.1073/pnas.93.26.15047

Vanlandschoot, P., Beirnaert, E., Neirynck, S., Saelens, X., Jou, W. M., & Fiers, W. (1996). Molecular and immunological characterization of soluble aggregated A/Victoria/3/75 (H3N2) influenza haemagglutinin expressed in insect cells. *Archives of Virology*, *141*(9), 1715–1726. https://doi.org/10.1007/bf01718294

Webb, S. R., Smith, S. E., Fried, M. G., & Dutch, R. E. (2018). Transmembrane domains of highly pathogenic viral fusion proteins exhibit trimeric association in vitro. *mSphere*, *3*(2), e00047–00018. https://doi.org/10.1128/mSphere.00047-18

Wuu, J. J., & Swartz, J. R. (2008). High yield cell-free production of integral membrane proteins without refolding or detergents. *Biochimica et Biophysica Acta/General Subjects*, *1778*(5), 1237–1250. https://doi.org/10.1016/j.bbamem.2008.01.023

Zhang, S., Wang, W. L., Chen, S., Lu, M., Go, E. P., Steinbock, R. T., Ding, H., Desaire, H., Kappes, J. C., Sodroski, J., & Mao, Y. (2018). Structural insights into the conformational plasticity of the full-length trimeric HIV-1 envelope glycoprotein precursor. *bioRxiv*, 288472. https://doi.org/10.1101/288472

Zoonens, M., Catoire, L. J., Giusti, F., & Popot, J. L. (2005). NMR study of a membrane protein in detergent-free aqueous solution. *Proceedings of the National Academy of Sciences of the United States of America*, *102*(25), 8893–8898. https://doi.org/10.1073/pnas.0503750102

Zoonens, M., Comer, J., Masscheleyn, S., Pebay-Peyroula, E., Chipot, C., Miroux, B., & Dehez, F. (2013). Dangerous liaisons between detergents and membrane proteins. The case of mitochondrial uncoupling protein 2. *Journal of the American Chemical Society*, *135*(40), 15174–15182. https://doi.org/10.1021/ja407424v

Zoonens, M., & Miroux, B. (2010). Expression of membrane proteins at the *Escherichia coli* membrane for structural studies. In I. Mus-Veteau (Ed.), *Heterologous expression of membrane proteins: Methods and protocols* (pp. 49–66). Humana Press.

SUPPORTING INFORMATION

Additional Supporting Information may be found online in the supporting information tab for this article.

How to cite this article: Clénet, D., Clavier, L., Strobbe, B., Le Bon, C., Zoonens, M., & Saulnier, A. (2021). Full-length G glycoprotein directly extracted from rabies virus with detergent and then stabilized by amphipols in liquid and freeze-dried forms. *Biotechnology and Bioengineering*, 118, 4317–4330. https://doi.org/10.1002/bit.27900